EPJ Web of Conferences **136**, 02005 (2017) DOI: 10.1051/epjconf/201713602005
RICAP16

Nuclei Measurements with the Alpha Magnetic Spectrometer on the International Space Station

Melanie Heil[1a]

[1]*Massachusetts Institute of Technology, 77 Massachusetts Avenue, Cambridge, MA 02139-4307*

Abstract. The exact behavior of nuclei fluxes in cosmic rays and how they relate to each other is important for understanding the production, acceleration and propagation mechanisms of charged cosmic rays. Precise measurements with the Alpha Magnetic Spectrometer on the International Space Station of light nuclei fluxes and their ratios in primary cosmic rays with rigidities from GV to TV are presented. The high statistics of the measurements require detailed studies and in depth understanding of associated systematic uncertainties.

1 Introduction

The Alpha Magnetic Spectrometer (AMS) is a multi-purpose magnetic spectrometer measuring cosmic rays up to TeV energies on the International Space Station (ISS). Its precision, large acceptance and ability to identify particle types over a large energy scale during its long duration mission make it unique in astro-particle physics. The AMS detector [1] consists of a transition radiation detector (TRD) [2], a silicon tracker [3], a permanent magnet, a Time-of-Flight detector (TOF) [4], a Ring Imaging Cherenkov detector (RICH) [5] and an electromagnetic calorimeter (ECAL) [6]. With these detectors AMS identifies particles and nuclei by redundant measurements of their charge and energy or momentum. In its first 5 years onboard the ISS AMS has recorded over 80 billion events. To match these statistics, detailed systematic error studies are important.

2 Particle Identification

Particle types are identified by charge measurements along the particle trajectory inside AMS. Redundant measurements by tracker, TOF, TRD, RICH and ECAL allow for precise particle identification. The best charge resolution is achieved by the combination of the seven inner tracker planes, which give a charge resolution of $\Delta Z = 0.05$ for protons and $\Delta Z = 0.07$ for Helium.

The TOF measures the particle velocities with a resolution of $\Delta\beta/\beta^2$ of 4% for protons and 2% for Helium. It thereby discriminates between upward and downward going particles. For our flux measurements only downward going particles are selected.

[a] Corresponding author: melanie.heil@cern.ch

The tracker together with the magnet determines the rigidity (momentum/charge) of the particles. The coordinate resolution in the bending direction is 10 μm and 7.5 μm for protons and helium, respectively. With this resolution we obtain a maximum detectable rigidity of 2 TV for protons and 3.2 TV for Helium using the full 3m lever arm of the tracker. In order to increase the statistics of the measurement for Z>2 nuclei, for rigidities below 1 TV we also analysed particles crossing only tracker planes L1 to L8 by which we gain a significant increase in acceptance.

3 Flux Measurements and Results

The isotropic particle or nuclei flux Φ_i for the ith rigidity bin (R_i , $R_i + \Delta R_i$) is

$$\Phi_i = N_i / (A_i \, \varepsilon_i \, T_i \, \Delta R_i) \quad (1)$$

where N_i is the number of events corrected for the bin-to-bin migration with the rigidity resolution function, A_i is the effective acceptance, ε_i is the trigger efficiency, and T_i is the collection time. The AMS fluxes [7,8] and flux ratios [9] were measured in bins chosen according to the tracker resolution function and available statistics. While the proton and Helium flux where determined with data collected in the first 30 month of data taking of AMS on the ISS, the Boron-to-Carbon ratio (B/C) was measured based on events collected in the first 5 years.

The effective acceptance A_i was calculated using Monte Carlo samples and then corrected for small differences found between the data and Monte Carlo event selection efficiencies, such as the efficiencies of track and beta measurement quality cuts. The trigger efficiency ε is measured from data with the unbiased trigger events. The trigger efficiency of protons ranges from 90 to 95% [7], while the trigger efficiency for helium and higher charge nuclei is well above 95% [8,9]. The bin-to-bin migration of events was corrected using the rigidity resolution functions obtained from Monte Carlo simulations [7-9].

Extensive studies were made of the systematic errors. The errors include the uncertainties in the trigger efficiency, the acceptance, the background contamination also accounting for interactions in the detector, the geomagnetic cutoff factor [10], the event selection, the unfolding, the rigidity resolution function, and the absolute rigidity scale.

The trigger efficiency error is dominated by the statistics available from the 1% prescaled unbiased event sample [7-9]. It is negligible (less than 0.2%) below 500 GV and reaches 1.5% at 1.8 TV for protons and 1% at 3 TV for helium and nuclei. The geomagnetic cutoff factor was varied from 1.0 to 1.4 and the resulting fluxes showed a systematic uncertainty of 2% at 1 GV and negligible above 2 GV.

As discussed above, the effective acceptance was corrected for small differences between the data and the Monte Carlo samples related to the event reconstruction and selection. The total corrections are less than 5% over the whole rigidity range, while the corresponding systematic uncertainties are less than 1% above 2 GV for protons and less than 2 % for helium and nuclei.

To accurately determine the acceptance of protons, helium and nuclei, their interactions with the detector materials have to be studied. The detector is mostly made of carbon and aluminum. For protons the corresponding inelastic cross-sections of p+Cand p+Al are known within better than 10%. To estimate the systematic error of the proton flux due to the uncertainty in the inelastic cross sections, dedicated samples of protons were simulated with the p + C and p+Al cross sections varied by ±10%. From the analysis of these samples together with the current knowledge of the cross sections, a systematic error of less than 1% was obtained. The inelastic cross sections of nuclei (Z>1) with Carbon and Aluminum have, if at all, only been measured below 10 GV. To accurately determine the effect on the acceptance of nuclei interactions in the detector, we have developed a method to determine the magnitude and rigidity dependence of the survival probability of the nuclei when traversing the detector materials. For this we used a sample of primary cosmic rays collected with AMS horizontal, that is, when the ISS was oriented such that AMS was pointing within $90^\circ \pm 10^\circ$ of the local zenith [8]. Using the measured interaction probabilities and, in addition, above 100 GV the rigidity dependence of the cross sections from the Glauber-Gribov model, the systematic error on

the flux due to uncertainties of nuclei inelastic cross sections was evaluated to be below 2% over the entire rigidity range.

The rigidity resolution function for protons was verified with data from both the ISS and the test beam and compared to the simulated events [7]. The rigidity resolution function for Z>1 nuclei is similar to that of protons. It was obtained from the simulations and extensively verified with the data [8, 9]. First, the differences of the coordinates measured in the inner tracker layers to those obtained from the track fit excluding the tested layer were compared between data and simulation. Second, the differences between the coordinates measured in L1 and L9 and those obtained from the track fit using the information from only the inner tracker were compared between events in data and simulation. The systematic errors on the fluxes due to uncertainties in the rigidity resolution function were obtained by varying the width of the Gaussian core of the resolution function and the amplitude of the non-Gaussian tails by their corresponding uncertainty over the entire rigidity range in the unfolding procedures. They were found to be small below 400 GV and reached 3.5% to 5% at the highest measured rigidities.

There are two contributions to the systematic uncertainty on the rigidity scale. The first is due to residual tracker misalignment. For the ISS data this error was estimated by comparing the E/p ratio for electron and positron events, where E is the energy measured with the ECAL and p is the momentum measured with the tracker [7]. It was found to be 1/26 TV^{-1}, limited by the current high-energy positron statistics. The second systematic error on the rigidity scale arises from the magnetic field map measurement and its temperature corrections and amounts to less than 0.5% for rigidities above 2 GV.

The contributions of individual sources to the systematic errors are added in quadrature to arrive at the total systematic uncertainty of the proton and helium flux. The Monte Carlo event samples have sufficient statistics such that they do not contribute to the errors.

To ensure that the treatment of systematic errors described above is correct, we performed several additional independent verifications. We checked that there is no dependence of the integral of the fluxes above 30 GV, *i.e.,* above the maximum geomagnetic cutoff, on the angle θ between the incoming particle direction and the AMS z-axis; this verifies the systematic errors assigned to the acceptance. We verified that the monthly integral fluxes above 45 GV are within the systematic errors; this verifies that the detector performance is stable over time. We checked that the ratios of fluxes obtained using events which pass through different sections of L1 to the average flux is in good agreement and within the assigned systematic errors; this verifies the errors assigned to the tracker alignment. Lastly, we verified that the fluxes obtained using the rigidity measured by only the inner tracker are in good agreement with the fluxes measured using the full lever arm. The flux ratios use the two different event samples corresponding to the inner tracker acceptance and to the L1 to L9 acceptance used for the results presented here. This verifies the systematic errors from the acceptance, the unfolding procedure, and the rigidity resolution function.

Figure 1(a) shows the proton flux as a function of rigidity with the total errors [7]. In this and the subsequent figures, the points are placed along the abscissa at the bins mean rigidity $\tilde{R}$ calculated for a flux $\propto R^{-2.7}$. Figure 1(b) shows the helium flux as a function of rigidity with the total errors [8].

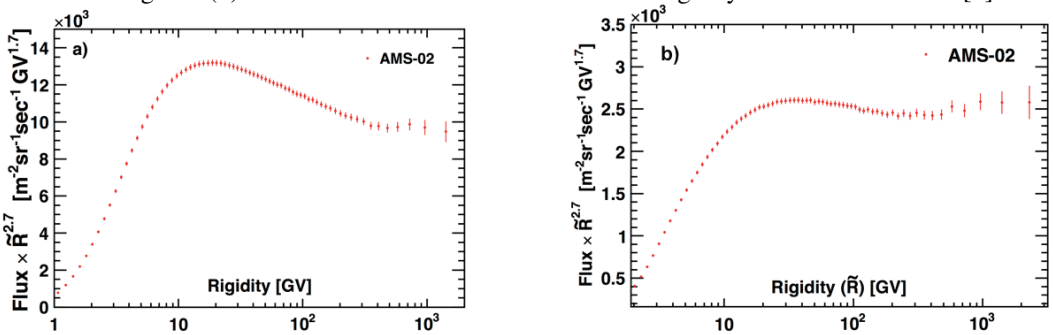

Figure 1. a) AMS proton flux and b) AMS Helium Flux, both multiplied by $R^{-2.7}$ for illustration purposes.

A power law with a constant spectral index does neither fit the proton flux nor the helium flux at the 99.9% C.L. for $R > 45$ GV. Instead a description with a double power law and a smooth transition between the two power laws describes the data well with the transition rigidity between 250 GV and 350 GV. Figure 2 a) shows the spectral indexes of the proton and the helium flux as a function of independent rigidity intervals and Figure 2 b) show the proton/helium ratio as a function of rigidity together with a single power law fit above 45 GV.

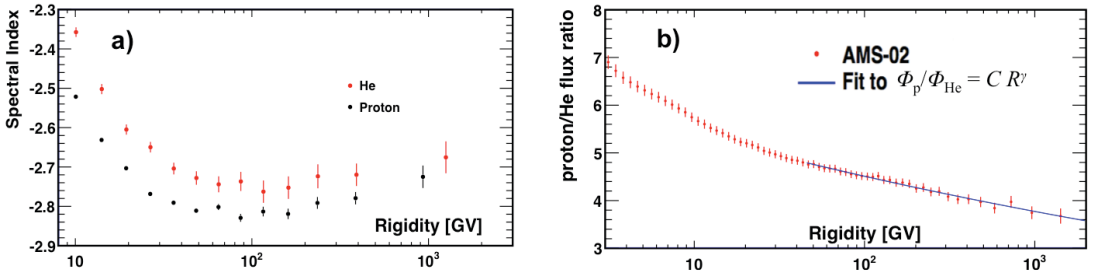

Figure 2. a) The spectral indexes of the AMS proton and helium fluxes. b) The AMS proton/helium ratio with a single power law fit above 45 GV.

Figure 3 shows the AMS result on B/C [9] as a function of rigidity with total errors. The B/C ratio is well described by a single power law above 65 GV with an index of -0.333.

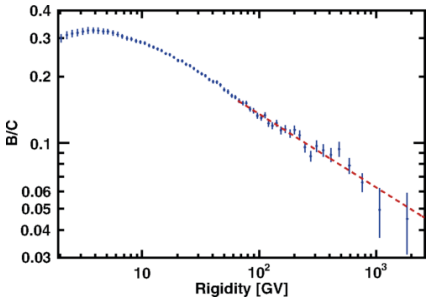

Figure 3. The AMS B/C ratio as a function of rigidity with a single power law fit above 65 GV.

4 Conclusions

The AMS results for protons, helium and B/C are reaching an unprecedented accuracy of ~1% for cosmic ray measurements. These precise measurements of different types of cosmic rays require a comprehensive model to describe all of their behaviour at the same time.

References

1. M. Aguilar *et al.,* Phys.Rev.Lett. **110,** 141102 (2013), and references therein.
2. Th. Kirn *et al.,* Nucl. Instrum. Methods Phys. Res., Sect. A **706**, 43 (2013).
3. B. Alpat *et al.,* Nucl. Instrum. Methods Phys. Res., Sect. A **613**, 207 (2010).
4. V. Bindi *et al.,* Nucl. Instrum. Methods Phys., Sect. A **743**, 22 (2014).
5. M. Aguilar-Benitez *et al*., Nucl. Instrum. Methods Phys. Res., Sect. A **614**, 237 (2010).
6. C. Adloff *et al*., Nucl. Instrum. Methods Phys. Res., Sect. A **714**, 147 (2013).
7. M. Aguilar *et al.,* Phys.Rev.Lett. **114,** 171103 (2015), and references therein.
8. M. Aguilar *et al.,* Phys.Rev.Lett. **115,** 211101 (2015), and references therein.
9. M. Aguilar *et al.,* Phys.Rev.Lett. **117,** 231102 (2016), and references therein.
10. D.F. Smart, M. A. Shea, Advances in Space Research **36,** 2012–2020 (2005).